Evolution of microstructure and properties of high-strength and high-conductivity Cu-(1~6wt.%) Ag alloy with eutectic structure

Yadong Ru[a], Zhongyuan Zhang[a,b], Tingting Zuo[a], Jiangli Xue[a], Zhaoshun Gao[a,c*], Lin zhang[d], Bo Da[e], Yongsheng Liu[b], Liye Xiao[a,c]

a. Institute of Electrical Engineering, Chinese Academy of Sciences, Beijing 100190, China

b. Department of physics, Shanghai university of electric power, Shanghai 201306, China

c. University of Chinese Academy of Sciences, Beijing 100049, China

d. College of Materials Science and Engineering, Chongqing University, Chongqing, 400044, China

e. Research and Services Division of Materials Data and Integrated System, National Institute for Materials Science, Tsukuba, 305-0047, Japan

Abstract

The Cu-(1~6 wt.%) Ag alloys with high strength and high conductivity were prepared by melting, forging and wire drawing in this paper. The evolution of microstructure and properties of the alloy during plastic deformation was studied. The results show that non-equilibrium eutectic colonies exist in the microstructure of Cu-(3~6 wt.%)Ag alloy and no eutectic colonies in the microstructure of Cu-(1~2 wt.%)Ag alloy. These eutectic colonies are arranged in parallel along the drawing direction during drawing and the size is refined with the increase of deformation strain. Attribute to the refinement of eutectic colonies, the Cu-Ag alloy exhibits higher strength with the increase of drawing strain.

Keywords: Cu-Ag alloy, high strength and high conductivity, microstructure, eutectic structure, strengthening mechanism

1. Introduction

The conductor material for the high field magnets is required to have high strength and high conductivity to overcome the huge electromagnetic stress and Joule heating[1, 2]. Cu-Ag alloy is one of the best conductor materials due to its high strength and high conductivity for high field magnets[3-5]. It is of great value and practical significance to further improve the strength and conductivity of Cu-Ag alloy for obtaining higher limit magnetic field strength. However, it is difficult to obtain Cu-Ag alloy with high strength and high conductivity simultaneously due to the contradictory relationship between the strength and conductivity[5-7].

The strength and electrical conductivity of Cu-Ag alloy are closely related to its microstructure and affected by Ag content[8, 9]. When the Ag content in Cu-Ag alloy exceeds 6 wt.%, the eutectic structure usually occurs in the microstructure[10, 11]. Then, the eutectic structure can be refined by severe plastic deformation and leading to a good strengthening effect[12-14]. However, too many eutectic interfaces will result in enhanced scattering of electrons and reduces the conductivity of the alloy significantly [14, 15]. When the Ag content in Cu-Ag alloy is less than 6%, there is generally no eutectic structure formed, and the alloy strength is mainly improved by aging precipitation and grain refinement[16, 17]. Whereas, only relying on these two strengthening mechanisms, the work hardening ability of Cu-Ag alloy is weakened at high deformation strains[7, 8, 18]. Therefore, it is necessary to control the eutectic structure and precipitated phase in Cu-Ag alloy by composition design and optimization of preparation process, so as to reduce the interface scattering and improve the work hardening ability of alloy simultaneously and obtain Cu-Ag alloy with high strength and high conductivity.

It is noted that a certain amount of eutectic structure can be obtained in alloys with lower solute content than eutectic composition during non-equilibrium freezing process [19, 20]. Therefore, it is proposed that the strength can be improved through obtaining non-equilibrium eutectic structure in Cu-Ag alloy with less than 6% Ag content. By coupling the eutectic structure and precipitated phase, high strength and

conductivity can be obtained at the same time. However, there are few studies on non-equilibrium eutectic structure in Cu-Ag alloys with low Ag content, and the changes of microstructure and their effects on properties are still unclear. In this paper, Cu-Ag alloy ingot with 1~6 wt.% Ag content was prepared by vacuum induction melting and furnace cooling. Then, through subsequent aging treatment, forging, rolling and cold drawing deformation, Cu-Ag alloy wire with high strength and high conductivity was obtained. The evolution of microstructure, strength and electrical conductivity of Cu-Ag alloys with different Ag contents during the preparation process were investigated.

2. Materials and methods

High-purity copper (99.9%) and silver (99.9%) were melted in a graphite crucible by vacuum induction melting and furnace cooling to obtain Cu-(1~6 wt.%) Ag alloy bars of 22 mm in diameter. Solution treatment was then carried out at 780℃ for 2 hours, followed by water quenching. The sample was cold forged to obtain the bar with a diameter of 14 mm, and then aged at 450℃ for 10 h. After aging treatment, the rod with a diameter of 8 mm was obtained through cold forging, and then the sample was cold-drawn to obtain the wire with a diameter of 0.5 mm. The drawing strain was calculated by Ln (A_0/A), A_0 was the initial cross-sectional area, and A was the final cross-sectional area of the sample.

Scanning electron micrograph (SEM) and energy dispersive spectroscopy (EDS) observation were carried on Zeiss company scanning electron microscope. The microstructure of the composite was characterized using a JOEL 2100 transmission electron microscopy (TEM) operated at an accelerating voltage of 200 kV. The transmission electron microscope sample was first ground and polished, and then thinned with Gatan ion thinning equipment. The hardness was measured by hardness tester. Uniaxial tensile tests were performed by MTS tensile testing machine at the strain rate of 1×10^{-3} s^{-1} with the sample length of ~10 cm at room temperature. A four-point method was used to test the conductivity of the alloy at the temperature of 20 °C.

3. Results and discussion

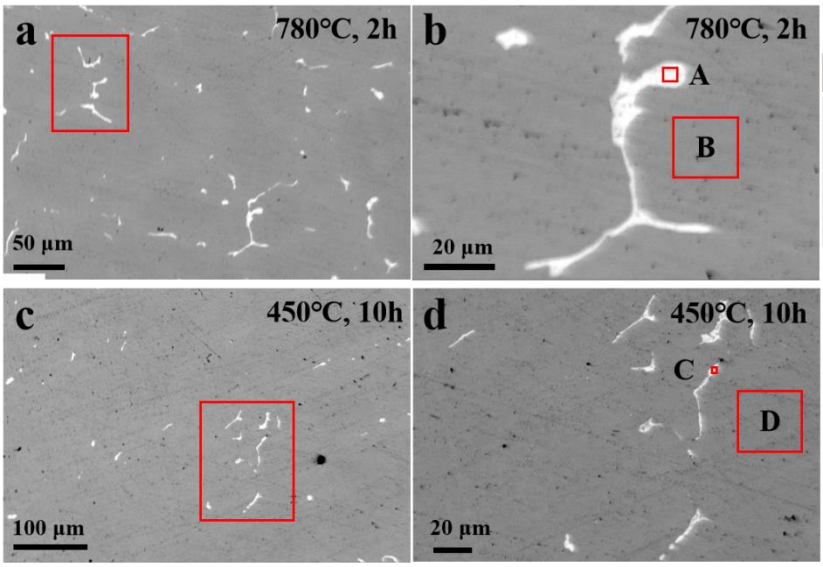

	Element	Weight%
A	Cu	33.53
	Ag	66.47
B	Cu	93.91
	Ag	6.09

	Element	Weight%
C	Cu	30.63
	Ag	69.37
D	Cu	95.76
	Ag	4.24

Fig.1. (a) Transverse cross-sectional SEM image of the Cu-6Ag alloy after solution treatment at 780℃ for 2 hours and water quenching. Supersaturated solid solution of Cu (dark) and eutectic colonies (bright) are present. (b) The magnified image of the box in Fig. 1a. The corresponding EDS results for the Cu-Ag alloys are shown on the right side of the Fig. 1b. (c) Transverse cross-sectional SEM image of the Cu-6Ag alloy after aging treatment at 450℃ for 10 hours. (d) The magnified image of the box in Fig. 1c. The corresponding EDS results for the Cu-Ag alloys are shown on the right side of the Fig. 1d.

Fig. 1a and 1b shows the transverse cross-sectional SEM image of the Cu-6Ag alloy after solution treatment at 780℃ for 2 hours and water quenching. The Cu-Ag alloys contained supersaturated solid solution of Cu (dark) and eutectic colonies (bright). The eutectic phase in the Fig.1a shows a strip island distribution with a width of about 4.5 μm. The results of energy spectrum of bright structure (point A) showed that Cu and Ag were 33.53 wt.% and 66.47 wt.% respectively. Due to the Ag content of Cu-Ag alloy is lower than the solid solubility limit of Ag solute in Cu matrix (7.9 wt.% Ag) at the eutectic temperature (779℃), it is considered that the non-equilibrium eutectic colonies (bright) were formed during non-equilibrium freezing process. The results of energy spectrum of dark structure (point B) showed that Cu and Ag were 93.91 wt.% and 6.09 wt.%, which exceeds the maximum solid solubility (0%) of Ag in Cu at room temperature, demonstrating the dark structure was supersaturated solid solution of Cu.

Fig. 1c and 1d shows the transverse cross-sectional SEM image of the Cu-6Ag alloy after aging treatment at 450℃ for 10 hours. Compared with the solution treatment state, the morphology of the eutectic colonies after aging annealing changes from strip island to small island, and the size of the eutectic colonies is refined to 3.7 μm, which should be related to the cold forging after solution. The role of solution treatment is to partially eliminate the ingrain segregation and make the coarse Ag redissolve into the Cu matrix as solid solution atoms. After the subsequent aging treatment at 450℃ for 10 h, the solid solution Ag atoms precipitate out of the matrix in the form of fine Ag-containing phase and the solid solubility in Cu matrix is reduced.

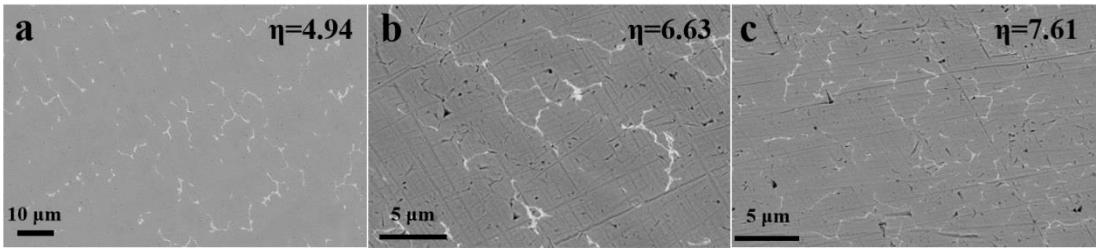

Fig.2. Transverse cross-sectional SEM image of the Cu-6Ag alloy with drawing strain of (a)4.94, (b)6.63 and (c)7.61.

Fig. 2 shows the transverse cross-sectional SEM image of the Cu-6Ag alloy during cold drawing. As can be seen, the eutectic colonies still present a discontinuous island distribution. The size of eutectic colonies decreases with the increase of drawing strain.

As the deformation increases, the size and morphology of eutectic colonies change. Fig. 3 shows the morphology and distribution of eutectic colonies of longitudinal section of Cu-6Ag alloy under drawing strains of 3.86, 4.43, 4.94, 6.63 and 7.61, respectively. When drawing strain η=3.86, some of eutectic colonies are at a certain angle with the drawing direction and are distributed in the shape of intermittent long island. While some are arranged in the parallel shape of long strip along the drawing direction, but their morphology is not strictly parallel with the drawing direction. The white bi-directional arrow indicates the cold drawing direction of the wire. With the increase of

deformation strain to η=4.43, the morphology of eutectic colonies changes greatly. The eutectic colonies oriented to the drawing direction with a low angle and the continuous long island distribution basically disappears, instead of the thin strip distribution along the drawing direction. After that, the eutectic colonies morphology does not change significantly with the increase of the drawing strain and the size is refined. When η=7.61, the eutectic colonies change into fine fiber strips parallel to the drawing direction. It is also worth noting that the eutectic colonies become more uniform with the increase of deformation when the size of eutectic colonies becomes smaller.

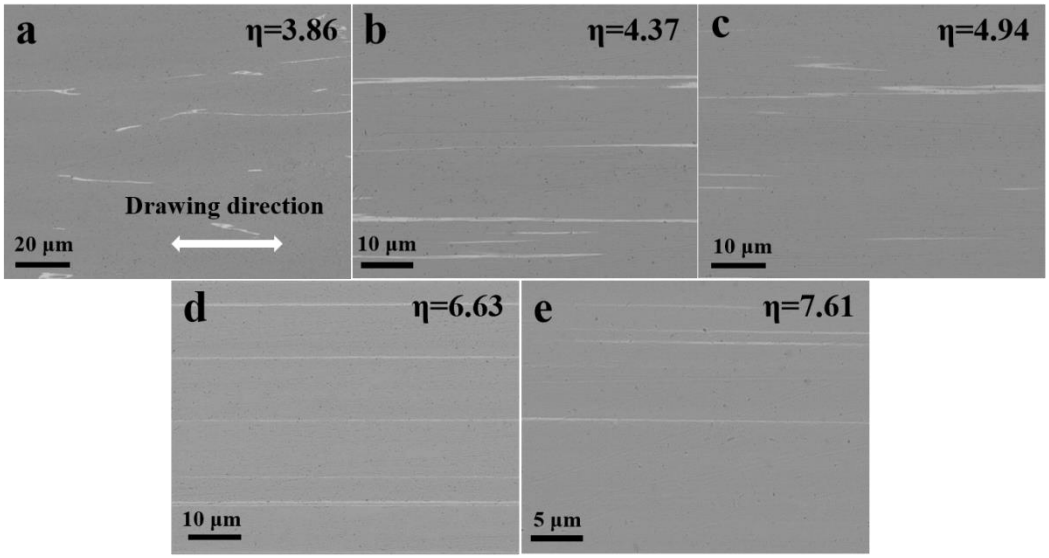

Fig.3. (a) Longitudinal SEM image of the Cu-6Ag alloy with drawing strain of (a)3.86, (b)4.43, (c)4.94, (d)6.63 and (e)7.61. The eutectic colonies (bright) were apparently refined.

Fig. 4 is the statistical results of the transverse size of eutectic colonies of longitudinal section of Cu-6Ag alloy different deformation strains corresponding to Figure 3. When η=3.86, the average eutectic colonies size is 1.047 μm as shown in Fig. 4a. The size distribution ranges from 0.25 μm to 2.5 μm and the eutectic phases with sizes less than 1 μm and larger than 1 μm occupy almost equal proportions. When the deformation is further increased to η=4.43, the average size of eutectic colonies size is 618 nm as shown in Fig. 4b. The proportion of eutectic colonies with a size greater than 1 μm is less than 20%, which is significantly lower than that when η=3.86. Fig. 4c shows the size

distribution of eutectic colonies when η=4.94. The average size of eutectic colonies is mainly distributed in the range of 100~900 nm, accounting for about 94%, and the average size is calculated to be 455 nm. When the drawing ratio increases to η=6.63, the average size of eutectic colonies is further refined to 241 nm. The histogram of size distribution is shown in Fig. 4d. When the drawing ratio increases to η=7.6, the average size of the eutectic fiber is 188 nm, as shown in Fig. 4e. Compared with the initial size distribution, the eutectic colonies size has been greatly refined from 1047 nm to 188 nm due to multiple passes of cold drawing. The change of average radial grain size with drawing strain is shown in Fig. 4f. On the other hand, the size distribution of eutectic fibers is more uniform and tends to refined to smaller size significantly.

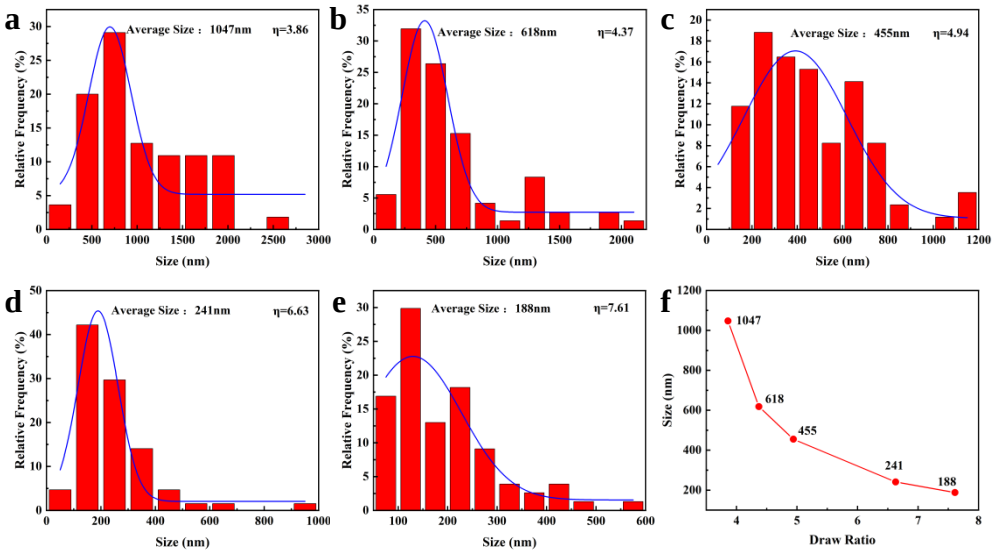

Fig.4. The average size statistics of the eutectic colonies in Cu-6Ag alloys with drawing strain of (a)3.86, (b)4.43, (c)4.94, (d)6.63 and (e)7.61. (f) The average size of the eutectic colonies as a function of the drawing ratio.

The microstructure evolution of Cu-6Ag alloy during cold drawing has been discussed above. The size of the non-equilibrium eutectic phase formed during the internal solidification of the alloy is refined with the increase of drawing deformation. The influence of Ag contents on the microstructure of Cu-Ag alloys with different will be analysed blow. Fig. 5 shows the longitudinal SEM images of Cu-Ag alloys with Ag contents of 2~5 wt.%. It can be seen that when the Ag

content in the alloy exceeds 3 wt.%, the eutectic fibers can be observed along the drawing direction in the Cu-Ag alloy. With the decrease of Ag content, the volume fraction of eutectic fibers decreases significantly. The distribution of eutectic fibers in Cu matrix becomes more uniform with the increase of drawing strain. These fine eutectic fibers distributed parallel to the drawing direction can improve the strength of the alloy. However, too many phase interfaces would increase the scattering of electrons and reduce the conductivity of the Cu-Ag alloy. It can be seen that no non-equilibrium eutectic fibers are observed in Cu-2Ag alloy in Fig.5d, which may be related to the low content of Ag in the Cu-Ag alloy and the small size of SEM samples. The atomic percentage of Ag in Cu-2Ag alloy is 1.2 at. %. After the solution treatment and aging treatment, these small number of Ag atoms may exist mainly in the Cu matrix as solid solution atoms or in the formation of nano precipitates, so the eutectic fibers of micron scale cannot be observed in the alloy. The nano precipitates in the alloy will be analyzed in detail later by TEM.

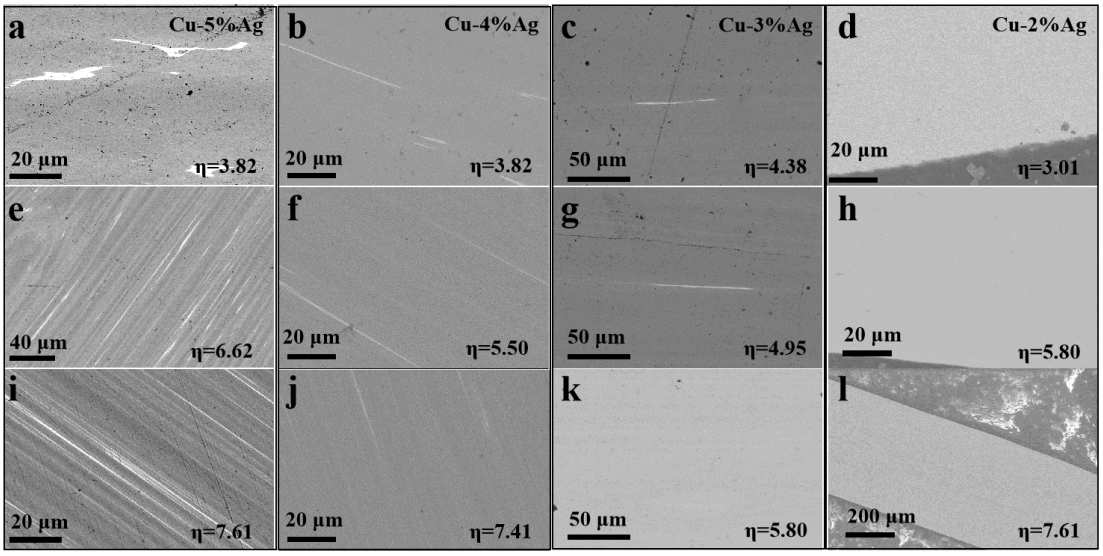

Fig.5. Longitudinal SEM image of the Cu-5Ag, Cu-4Ag, Cu-3Ag, Cu-2Ag alloy with different drawing strains.

Transmission electron microscopy was used to investigate the microstructure of the Cu-Ag alloy, so as to further analyze the strengthening mechanism of the alloy. The Cu-6Ag alloy and Cu-2Ag alloy were selected as the representatives

of the Cu-Ag alloy with and without eutectic structure, respectively. Fig. 6a-c is a TEM image of the longitudinal section of Cu-6Ag alloy at the drawing strain of η=7.61. The direction of the white bidirectional arrow in the figure is the drawing direction. It can be clearly seen that the microstructure of Cu-6Ag alloy after drawing is arranged in parallel along the drawing direction, and the strip grains is observed. As shown in Fig. 6b and 6c, the width of Ag fibers in the alloy is between 5 and 50 nm.

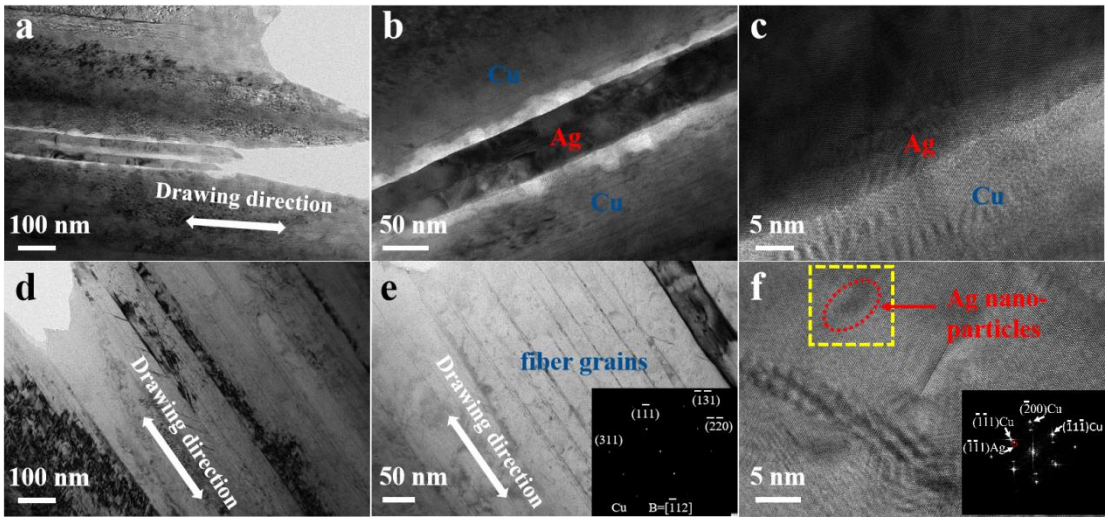

Fig.6. (a-c) Longitudinal TEM image of the Cu-6Ag alloy with drawing strain of 7.61. (b) bright field image shows the Cu grains and Ag fiber. (c) the high-resolution image of the Cu/Ag interface. (d-f) Longitudinal TEM image of the Cu-2Ag alloy with drawing strain of 7.61. (e) bright field image shows the fiber-like structure in Cu grains. (f) the high-resolution image of the Ag nano-particles.

Fig.6 d-f Shows the TEM image of the longitudinal section of Cu-2Ag alloy when the drawing ratio is η=7.61. After large drawing deformation, the grains extend along the drawing direction and the radial size is refined obviously. The white bi-directional arrow in Fig. 6d shows the direction of cold drawing. It shows obvious strain contrast and the dislocation distribution within the grains becomes very uneven. The dislocation density is very high in some grains, while the dislocation is almost invisible and the grain boundary cannot be clearly distinguished in other grains. The density of dislocation of the Cu-2Ag alloy is very low as shown in Fig. 6e. The grains were elongated and refined along the drawing direction, during which fine stripes were observed in the interfaces. The

selected area electron diffraction (SAED) shows that there is only Cu phase and no diffraction spots of Ag phase, which indicate that fine stripes may be related to the existence of large strain at the interface[20-23]. Fig. 6f shows a high resolution transmission electron microscopy (HRTEM) image of Cu-2Ag alloy when η=7.61. The diffraction spots of fast Fourier transform (FFT) results in the box area of yellow dotted line are shown in the lower left corner. The results showed that there were Cu and Ag diffraction spots in the region, indicating the presence of nano-sized Ag particles embedded in the Cu matrix.

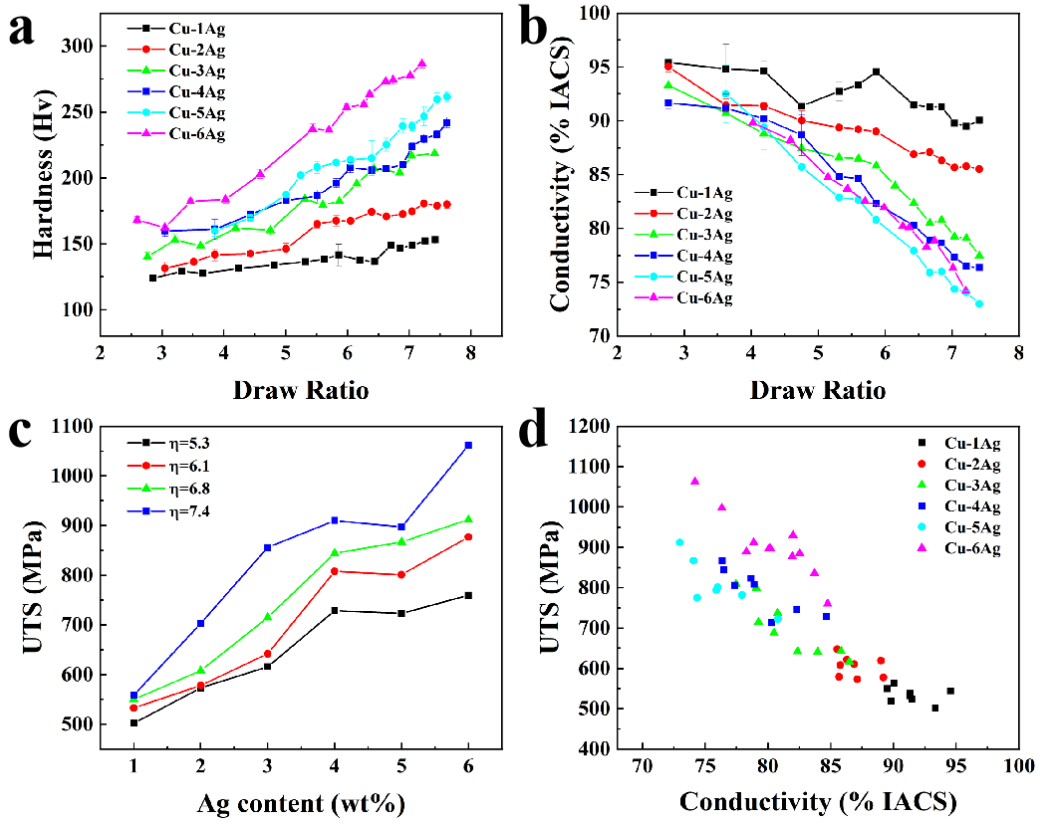

Fig.7. (a) Hardness and (b) conductivity of Cu-Ag alloys with 1~6 Ag content as a function of the drawing ratio. (c) Ultimate tensile strength of Cu-Ag alloys with different drawing ratio as a function of Ag content. (d) Relationship between strength and conductivity of the Cu-(1~6) Ag alloys.

Fig. 7a shows the variations of hardness of Cu-Ag alloy with different Ag contents as a function of drawing strain. The hardness of Cu-Ag alloy increases with the increase of drawing strain and Ag content. The hardness increased in obviously higher rate in Cu-(3~6)Ag alloys than Cu-(1~2)Ag alloys, which can

be explained by the microstructure evolution. When Ag content is higher than 3 wt.%, obvious eutectic colonies can be observed and the eutectic colonies was refined and become fibrous as drawing strain increased. It is indicated the strengthening of eutectic fiber makes the hardness increase faster in Cu-(3~6)Ag alloys than that of Cu(1~2)Ag alloys.

Fig. 7b shows the variations of conductivity of Cu-Ag alloys with different Ag contents as a function of drawing strain. Contrary to the trend of hardness change, the conductivity of Cu-Ag alloy decreases with the increase of drawing strain and Ag content. The electrical conductivity of Cu-(3~6)Ag alloys decreased more significantly than Cu(1~2)Ag alloys under the same deformation. In especial, the eutectic fiber is refined to about 100 nanometer and results in more interfaces at high deformation strains. These phase interfaces and grain boundaries significantly increases the scattering of electrons, which lead to the rapid decrease of Cu-Ag electrical conductivity under high deformation strains.

Fig. 7c shows the ultimate tensile strength of Cu-Ag alloys with different drawing strain as a function of Ag content. Similar to hardness, the tensile strength of Cu-Ag alloy increases with the increase of deformation. With the increase of deformation, the eutectic fiber and Cu matrix will be arranged in parallel along the drawing direction, and the size of the eutectic fiber will be refined and finally become the strip of fine fiber. Due to the size refinement of Cu matrix and eutectic fiber, the strength of the alloy increases with the increase of drawing deformation. Fig. 7d shows the relationship between strength and conductivity of the Cu-(1~6)Ag alloys. With the increase of Ag content and drawing strain, the strength of Cu-Ag alloy increases and electrical conductivity decreases. This proves that the contradictory relationship between strength and conductivity during cold deformation. By optimizing the Ag content and preparation process, the Cu-Ag alloy with better comprehensive properties can be obtained.

4. Conclusions

In this paper, Cu-(1~6 wt.%) Ag alloys wire has been obtained by vacuum induction smelting, heat treatment (solid solution treatment and aging treatment) and cold deformation processing. The eutectic phase aligned along the drawing direction and the average thickness of eutectic phase was refined from about 1.047 μm to 188 nm during drawing. Non-equilibrium eutectic was found in the Cu-(3~6)Ag alloy and absent in Cu-(1~2)Ag. The refined eutectic fiber significantly increases the strength of the alloys. Meanwhile, the electron scattering increased and electrical conductivity decreased due to the increasement of the interfaces. By coupling the eutectic structure and precipitated phase, the Cu-Ag alloy with excellent comprehensive properties was obtained.

Acknowledgements

The authors thank the Institute of Electrical Engineering, CAS (E155710301 and E155710201) for financial support. The authors would like to thank in particular Zhixiang Tang (Chongqing University) for valuable discussion and preparing of Cu-Ag wires.

Reference

[1] H.J. Schneider-Muntau, Pulsed monocoil magnets for highest fields, Current Applied Physics 6(1) (2006) 54-58.
[2] K. Spencer, F. Lecouturier, L. Thilly, Established and emerging materials for use as high–field magnet conductors, Advanced Engineering Materials 6(5) (2010) 290-297.
[3] Y. Sakai, K. Inoue, H.J.A.m.e.m. Maeda, New high-strength, high-conductivity Cu-Ag alloy sheets, 43(4) (1995) 1517-1522.
[4] J. Freudenberger, W. Grünberger, E. Botcharova, A. Gaganov, L. Schultz, Mechanical properties of cu-based micro and macrocomposites, Advanced Engineering Materials 4(9) (2010) 677-681.
[5] Y. Sakai, K. Inoue, T. Asano, H. Wada, H. Maeda, Development of high strength, highconductivity Cu–Ag alloys for high–field pulsed magnet use, Applied Physics Letters 59(23) (1991) 2965-2967.
[6] Y. Sakai, H.J. Schneider-Muntau, Ultra-high strength, high conductivity Cu-Ag alloy wires, Acta materialia 45(3)(1017-1023) (1997).
[7] Y.G. Ko, S. Namgung, B.U. Lee, D.H. Shin, Mechanical and electrical responses of nanostructured Cu–3 wt%Ag alloy fabricated by ECAP and cold rolling, Journal of

Alloys and Compounds 504 (2010) S448-S451.
[8] J.B. Liu, L. Meng, Y.W. Zeng, Microstructure evolution and properties of Cu–Ag microcomposites with different Ag content, Materials Science and Engineering: A 435-436 (2006) 237-244.
[9] G. Bao, Y. Xu, L. Huang, X. Lu, L. Zhang, Y. Fang, L. Meng, J. Liu, Strengthening effect of Ag precipitates in Cu–Ag alloys: a quantitative approach, Materials Research Letters 4(1) (2016) 37-42.
[10] M. Xie, W. Huang, H. Chen, L. Gong, B. Yang, Microstructural evolution and strengthening mechanisms in cold-rolled Cu–Ag alloys, Journal of Alloys and Compounds 851 (2020) 156893.
[11] Y. Tian, J. Li, P. Zhang, S. Wu, Z. Zhang, M. Kawasaki, T. Langdon, Microstructures, strengthening mechanisms and fracture behavior of Cu–Ag alloys processed by high-pressure torsion, Acta materialia 60(1) (2012) 269-281.
[12] A. Benghalem, D.G. Morris, Microstructure and strength of wire-drawn Cu-Ag filamentary composites, Acta Materialia 45(1) (1997) 397-406.
[13] S. Hong, M. Hill, Microstructural stability and mechanical response of Cu–Ag microcomposite wires, Acta materialia 46(12) (1998) 4111-4122.
[14] L. Zhang, L. Meng, Evolution of microstructure and electrical resistivity of Cu–12wt.%Ag filamentary microcomposite with drawing deformation, Scripta Materialia 52(12) (2005) 1187-1191.
[15] S.I. Hong, M.A. Hill, Mechanical stability and electrical conductivity of Cu–Ag filamentary microcomposites, Materials Science and Engineering: A 264(1-2) (1999) 151-158.
[16] X. Zhu, Z. Xiao, J. An, H. Jiang, Y. Jiang, Z. Li, Microstructure and properties of Cu-Ag alloy prepared by continuously directional solidification, Journal of Alloys and Compounds 883 (2021).
[17] B.B. Zhang, N.R. Tao, K. Lu, A high strength and high electrical conductivity bulk Cu-Ag alloy strengthened with nanotwins, Scripta Materialia 129 (2017) 39-43.
[18] K. Sitarama Raju, V. Subramanya Sarma, A. Kauffmann, Z. Hegedűs, J. Gubicza, M. Peterlechner, J. Freudenberger, G. Wilde, High strength and ductile ultrafine-grained Cu–Ag alloy through bimodal grain size, dislocation density and solute distribution, Acta Materialia 61(1) (2013) 228-238.
[19] J. Lin, L. Meng, Effect of aging treatment on microstructure and mechanical properties of Cu–Ag alloys, Journal of Alloys and Compounds 454(1-2) (2008) 150-155.
[20] J.B. Liu, L. Zhang, D.W. Yao, L. Meng, Microstructure evolution of Cu/Ag interface in the Cu–6 wt.% Ag filamentary nanocomposite, Acta Materialia 59(3) (2011) 1191-1197.
[21] S.I. Hong, M.A. Hill, Microstructural stability and mechanical response of Cu–Ag microcomposite wires, Acta materialia 46(12) (1998) 4111-4122.
[22] K.H. Lee, S.I. Hong, Interfacial and twin boundary structures of nanostructured Cu–Ag filamentary composites, Journal of materials research, 18(9) (2003) 2194-2202.
[23] J.B. Liu, L. Zhang, Y.W. Zeng, L. Meng, Co-deformation in Cu–6wt.% Ag

nanocomposites, Scripta Materialia 64(7) (2011) 665-668.